CHAPTER 3

INNERVATION OF THE NON-PREGNANT RAT UTERUS

Twenty-two rats in the estrous or estrous/diestrous stage of the estrous cycle provided tissue for this project. Non-pregnant uteri at other stages of the cycle were not examined. The average weight of non-pregnant uterine horns at the estrous/early diestrus stage was 0.21 $\pm$ 0.03 g (mean $\pm$ SD; n = 44 horns). Their mean area, mean length and mean width were 5.51 $\pm$ 0.73 cm^2, 6.12 $\pm$ 0.70 cm and 0.95 $\pm$ 0.09 cm, respectively.

Uterine horns from at least 6 non-pregnant rats were stained for each neurochemical localized in this project. For each neurochemical, both right and left uterine horns from one or two rats were stained to determine whether the innervation of the two horns was the same.

Anatomy of the uterine wall

Linea Uteri

Linea uteri are thick bundles of longitudinal smooth muscle that form a ridge opposite the mesometrium (Melton & Saldivar, 1967) and are surrounded by connective tissue (Borda et al., 1978). They have unique functional, pharmacological and morphological characteristics compared to the rest of the smooth muscle in the non-pregnant uterine horn (Borda et al., 1978). I found linea uteri in the three different rat strains that I examined, i.e., Sprague Dawley (Figure 3.1A), Hooded Wistar (Figure 3.1B) and Fisher 344 (Figure 3.1C). As shown in Figure 1 and noted by Melton and Saldivar (1967), linea uteri are visible to the naked eye. It is therefore surprising that the presence of linea uteri has not been mentioned in any of the studies on the innervation of the rat uterus,

FIGURES 3.1A-3.1C Linea Uteri *in vivo*

Linea uteri are visible to the naked eye in the non-pregnant rat uterus. Linea uteri (arrows) were found in Sprague Dawley (A), Fisher 344 (B) and Hooded Wistar (C).

Linea Uteri

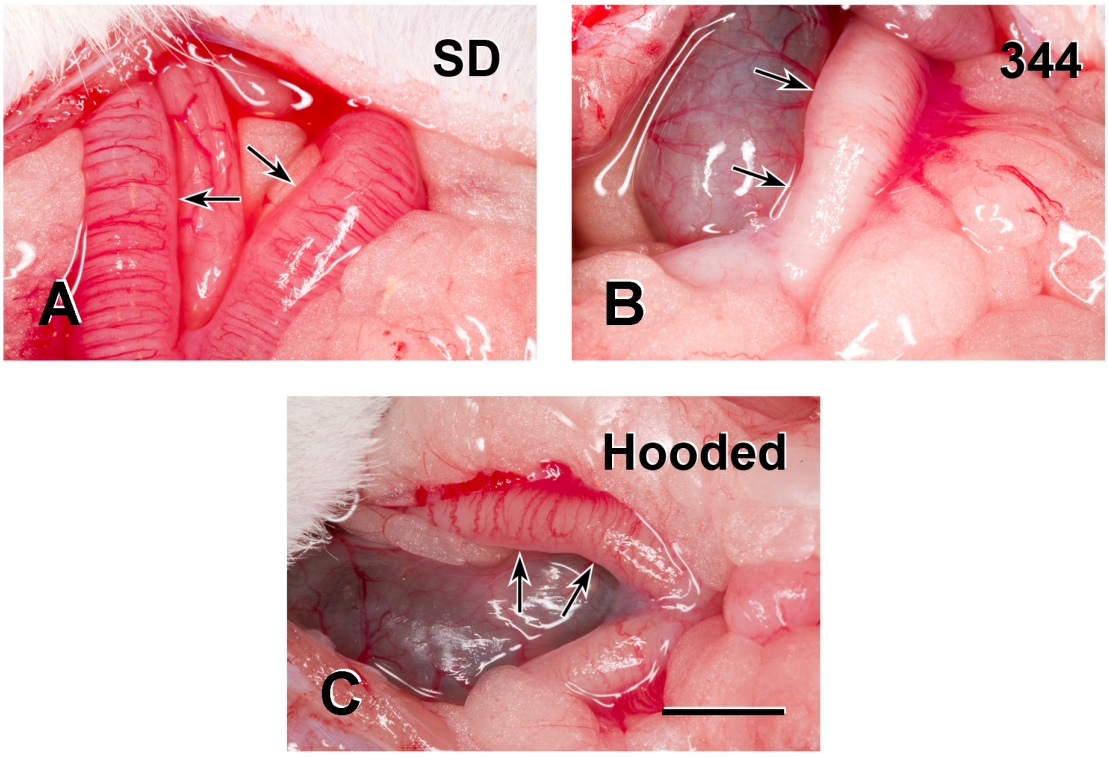

particularly since I found that the linea uteri were more densely innervated than other regions of the longitudinal smooth muscle.

Sympathetic Innervation of the non-pregnant rat uterus

Immunoreactivity for tyrosine hydroxylase (TH) and neuropeptide Y (NPY) were used to identify sympathetic nerves. Significant densities of both TH-immunoreactive axons and NPY-immunoreactive axons were found in the non-pregnant rat uterus at the estrous stage.

Tyrosine Hydroxylase (TH)

TH-immunoreactive axons were found in abundance around blood vessels in uterine horns from non-pregnant rats. Non-varicose TH fibers entered the uterus through the mesometrium in thick nerve bundles that lay alongside blood vessels. As the blood vessels branched within the uterus, their diameter decreased and the nerve bundles accompanying them became smaller and contained fewer TH-immunoreactive axons (Figure 3.2A). Whole mounts of non-pregnant uterine horns stained for TH and then embedded in paraffin and sectioned at 10 µm revealed that the TH axons were associated with arterioles and not veins (Figure 3.2B & 3.2C).

Innervation by TH axons was densest around blood vessels; endometrial TH innervation was less dense and the least dense TH innervation occurred in the myometrium.

TH innervation of the myometrium: TH-immunoreactive axons occurred in all regions of the myometrium. The linea uteri had a higher density of varicose TH-immunoreactive axons compared to the rest of the uterine smooth muscle (Figure 3.2F).

FIGURE 3.2A. Uterine whole mount stained for tyrosine hydroxylase (TH)

Whole mount preparation of the entire full thickness non-pregnant uterine horn stained for TH. Letters indicate the location of the micrographs shown in Figures 3-2D and 3-2E. Bar, 5 mm

TH : Estrous

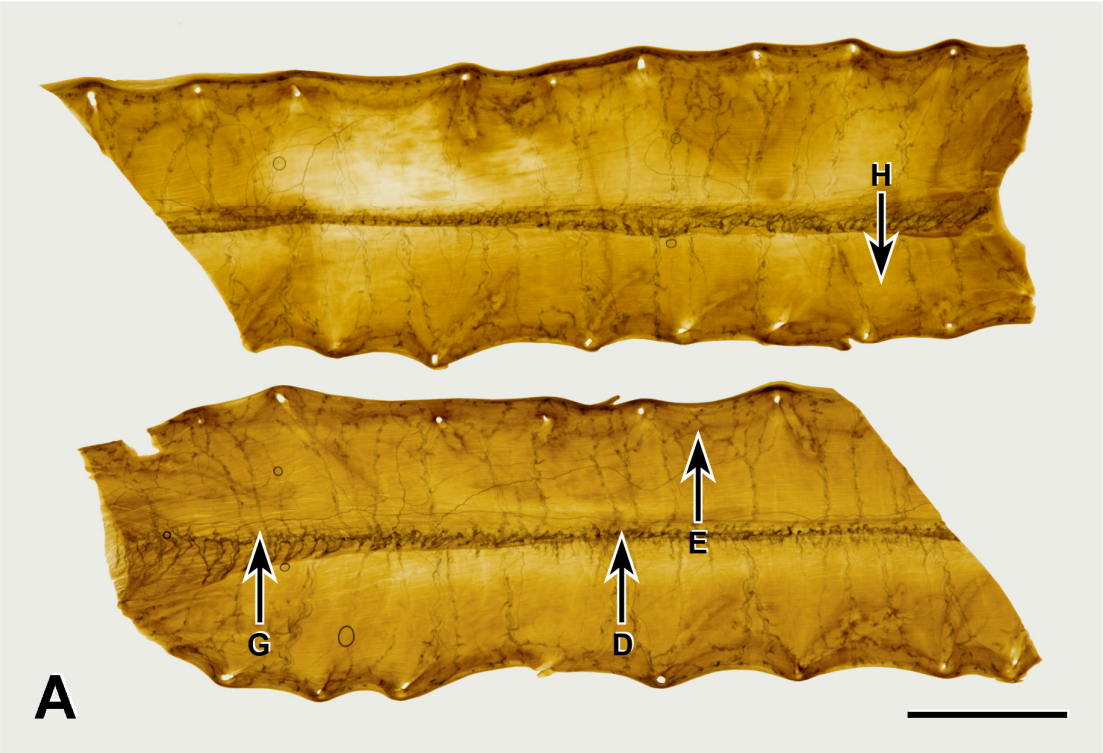

FIGURES 3.2B & 3.2C TH-immunoreactive axons in paraffin sections

B, Longitudinal section through a uterine whole mount that was stained for TH, embedded in paraffin, cut at 10 µm and then stained with haematoxylin and eosin. **C**, Section that is semi-serial to the section shown in B and that has not been stained with haematoxylin and eosin. Arrows indicate TH-positive axons that are part of the perivascular plexus around an arteriole that has been cut *en face*. V1 and V2 indicate veins cut in transverse section. TH-stained axons are associated with arterioles but not veins. Bar in C, 50 µm.

TH : Estrous

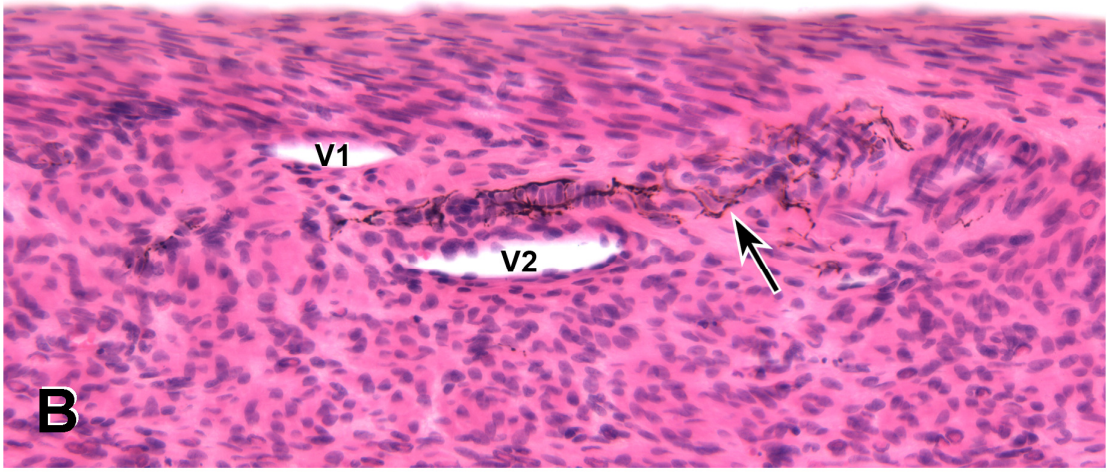

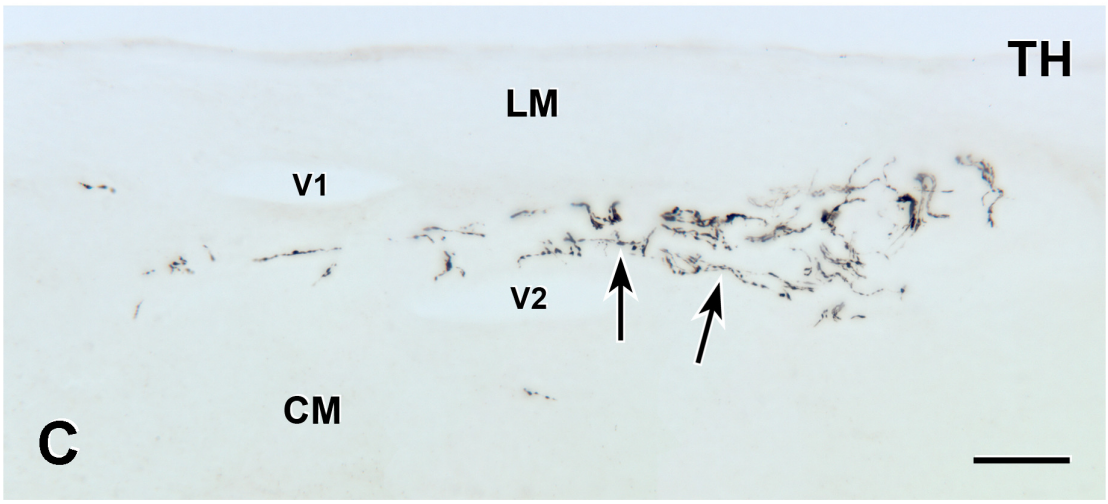

TH axons in the linea uteri and longitudinal and circular muscle layers were fine and varicose and ran parallel to the long axes of the smooth muscle cells, i.e. they were oriented predominantly longitudinally in the linea uteri and longitudinal muscle layer and predominantly circularly in the circular muscle layer. In the myometrium, the TH innervation consisted mainly of individual varicose immunoreactive axons but small nerve bundles containing a few varicose immuno-positive axons were also present

TH innervation of the endometrium: By the time that the blood vessels reached the endometrium, there were only a few TH-immunoreactive axons associated with each vessel. Many of these TH axons were varicose and followed a crooked path into the endometrium where they terminated. Rare varicose TH axons arose from the nerve bundles associated with blood vessels in the myometrium and travelled into the endometrium before entering the myometrium again to join an adjacent nerve bundle associated with a blood vessel. Rare varicose TH axons that arose from nerve bundles around blood vessels approached uterine glands in the endometrium (Figure 3.2H). Some TH axons took tortuous courses to reach the endometrium. They left nerve bundles around blood vessels in the myometrium and looped through many different focal planes before terminating deep in the endometrium. Thick nerve bundles that branched and contained many non-varicose and varicose TH-positive axons formed a loose network along the entire uterus (Figure 3.2G). These thick bundles were located mainly in the endometrium. On rare occasions, thinner nerve bundles arising from the thick bundles connected with the perivascular plexus around blood vessels in the endometrium.

The general organization of the TH innervation did not appear to differ between the mesometrial and anti-mesometrial sides of the uterus or between the ovarian, middle and cervical regions. If the density of innervation varied between these different uterine regions, the variation was not great enough to be visually apparent without quantification.

FIGURE 3.2D & 3.2E TH-immunoreactive axons associated with blood vessels

D, Montage of 3 different focal places showing TH-immunoreactive axons entering the uterus from the mesometrium along with blood vessels. Bar, 0.5 mm. **E**, Higher magnification micrograph showing the dense perivascular plexus of TH-positive axons around a blood vessel. The density of TH-stained axons in the plexus reduces when the blood vessel branches. Bar, 100 μm.

TH : Estrous

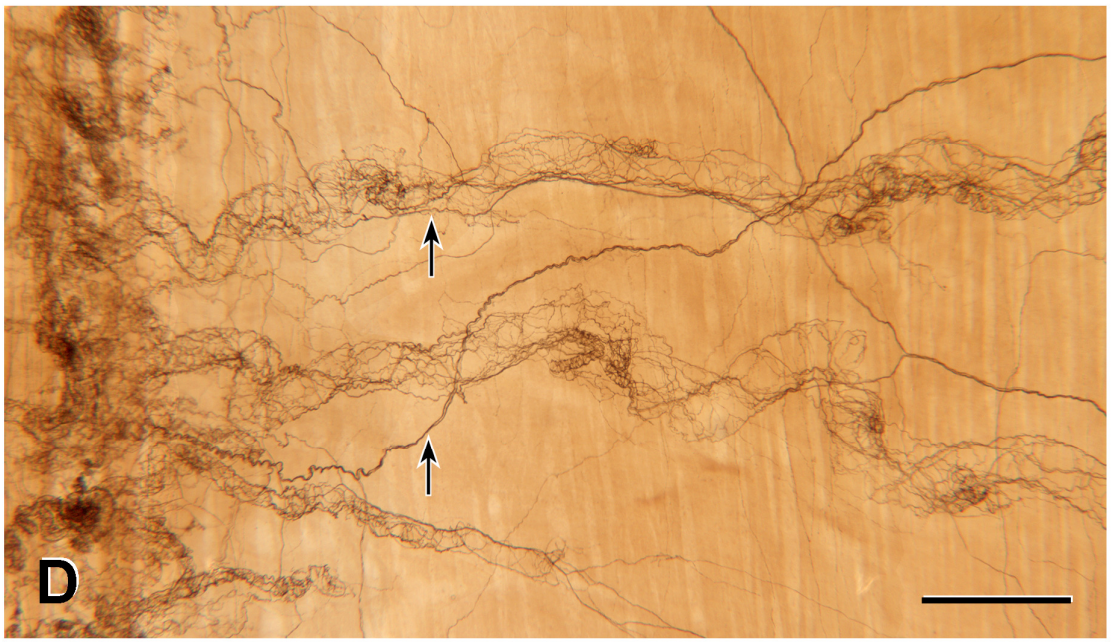

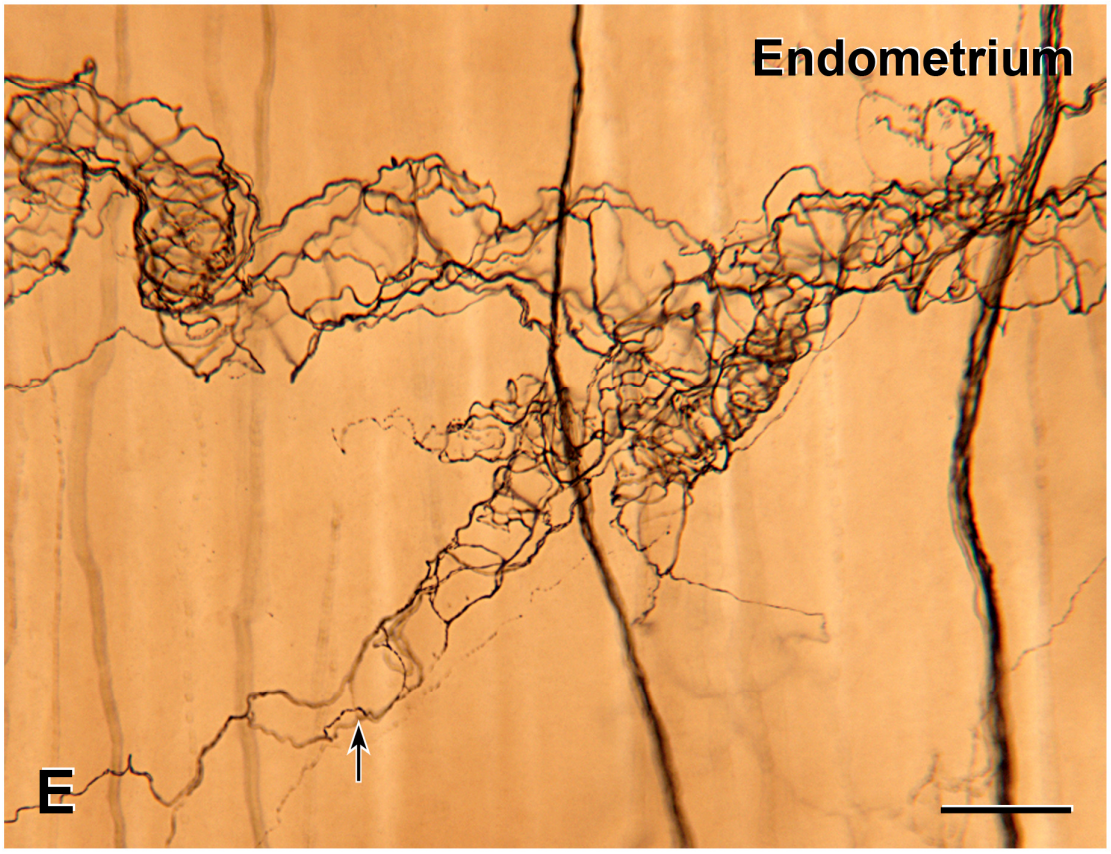

FIGURES 3.2F & 3.2G TH-immunoreactive axons in the linea uteri and endometrium

F, Dense innervation of the linea uteri by TH-containing axons (arrows). TH axons follow the orientation of the longitudinal smooth muscle cells. **G**, Thick nerve bundle that is very heavily stained for TH in the endometrium. Note that the bundle is not associated with blood vessels. Bars, 100μm

TH : Estrous

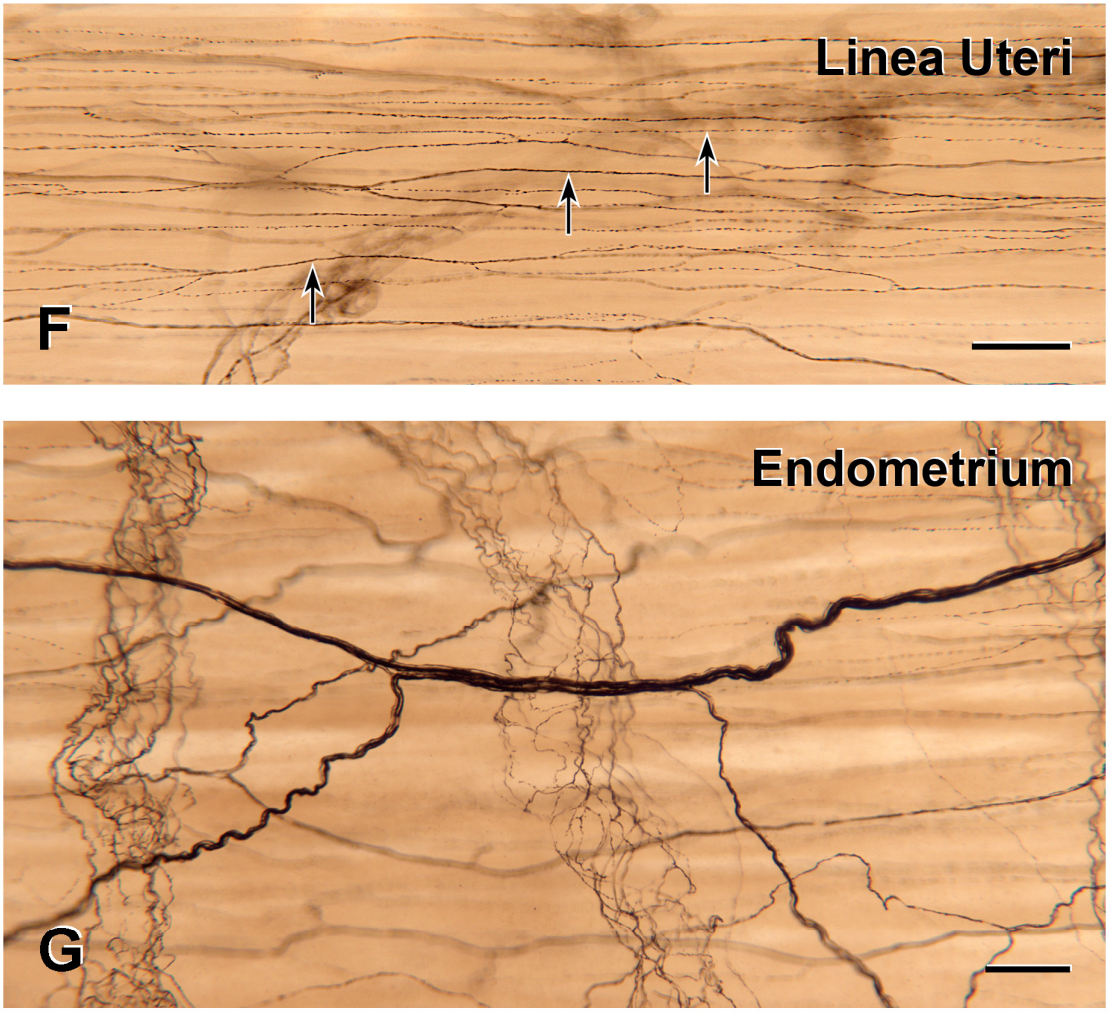

FIGURE 3.2H TH-immunoreactive innervation of uterine glands

TH-positive axons (arrow) travel close to a uterine gland deep in the endometrium. Bar, 100 μm.

TH : Estrous

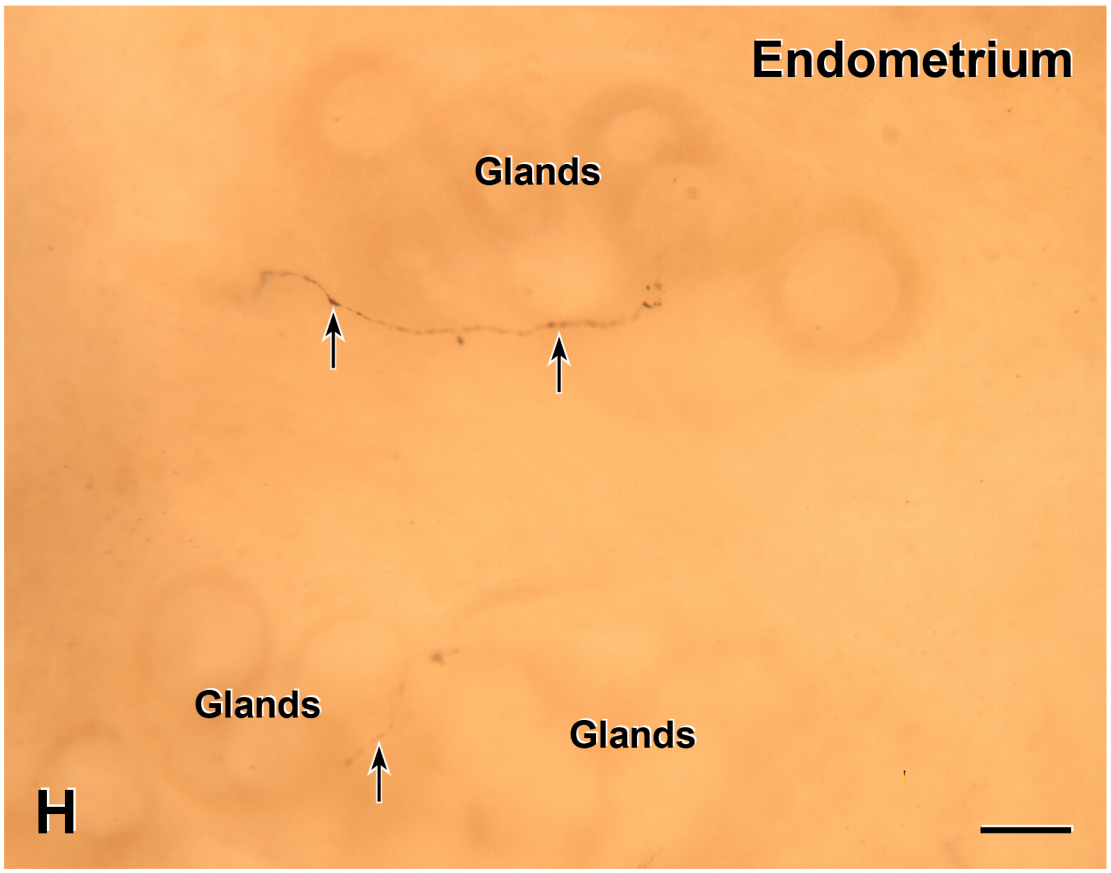

The right and left uterine horns from one non-pregnant rat were processed to reveal TH-immunoreactivity. Innervation did not differ between the right and left horns.

Neuropeptide Y (NPY)

Dense plexuses of non-varicose NPY-immunoreactive axons occurred around blood vessels in the non-pregnant rat uterus (Figure 3.3C). Non-varicose NPY-positive axons entered the uterus along with blood vessels at the mesometrium. The blood vessels decreased in diameter as they branched and the accompanying nerve bundles also showed a reduction in the number of NPY-immunoreactive axons (Figure 3.3A). Some varicose NPY axons travelled from nerve bundles associated with one blood vessel to a nerve bundle that was associated with another blood vessel. . Nerve bundles that contained non-varicose NPY-immunoreactive axons and were associated with blood vessels formed a network throughout the entire length of the uterus (Figure 3.3A). NPY axons followed the branches of blood vessels less far than TH axons so that the plexuses of NPY-immunoreactive axons around small vessels often appeared to terminate abruptly (Figure 3.3D). The perivascular NPY innervation associated with blood vessels appeared to be less dense than the perivascular TH innervation.

NPY axons most densely innervated blood vessels with innervation less dense in the endometrium and least dense in the myometrium.

<u>NPY innervation of the myometrium</u>: Many varicose NPY-immunoreactive axons were found in all layers of the myometrium. The linea uteri had more varicose NPY-immunoreactive fibers than the rest of the uterine smooth muscle (Figure 3.3B). Like TH axons, NPY axons ran longitudinally in the linea uteri and longitudinal muscle and circularly in the circular smooth muscle. Fine varicose NPY axons were formed a regular pattern on the mesometrial side of the uterus (Figure 3. 3E) but were not encountered on

FIGURES 3.3A & 3.3B Uterine whole mount stained for NPY and NPY-positive axons in the linea uteri.

A, Whole mount preparation of the entire full thickness non-pregnant uterine horn stained for NPY. Letters indicate the location of the micrographs shown in Figures 3.3B, 3.3C, 3.3E and 3.3F. Bar, 5 mm. **B**, Varicose NPY-immunoreactive axons (arrows) in the linea uteri of the non-pregnant uterus. Bar, 250 µm.

NPY : Estrous

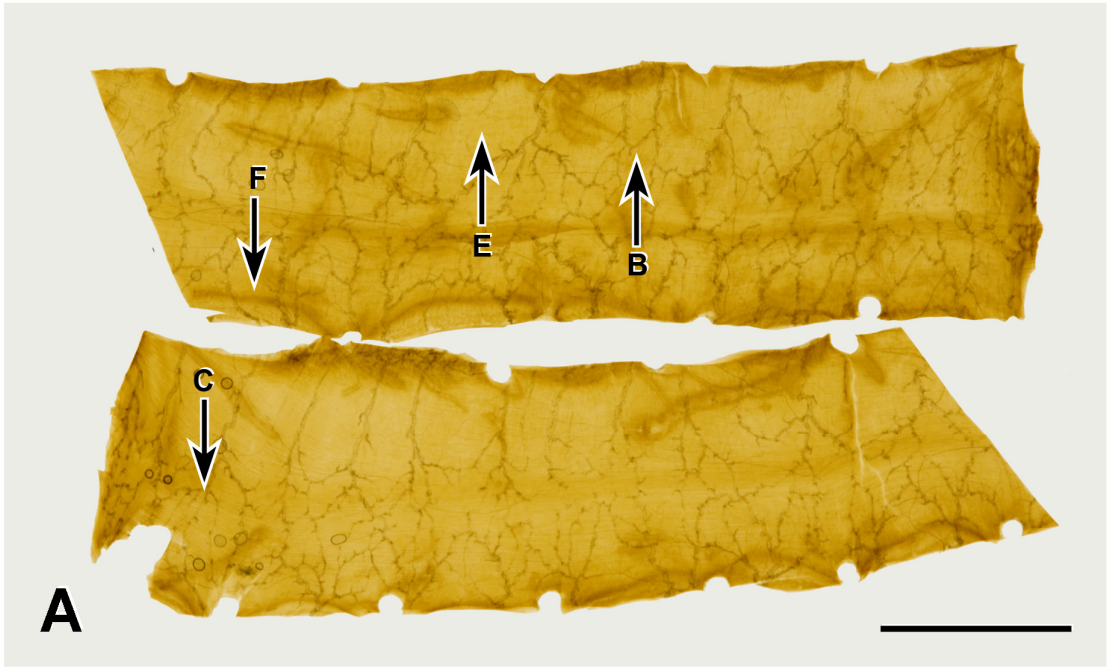

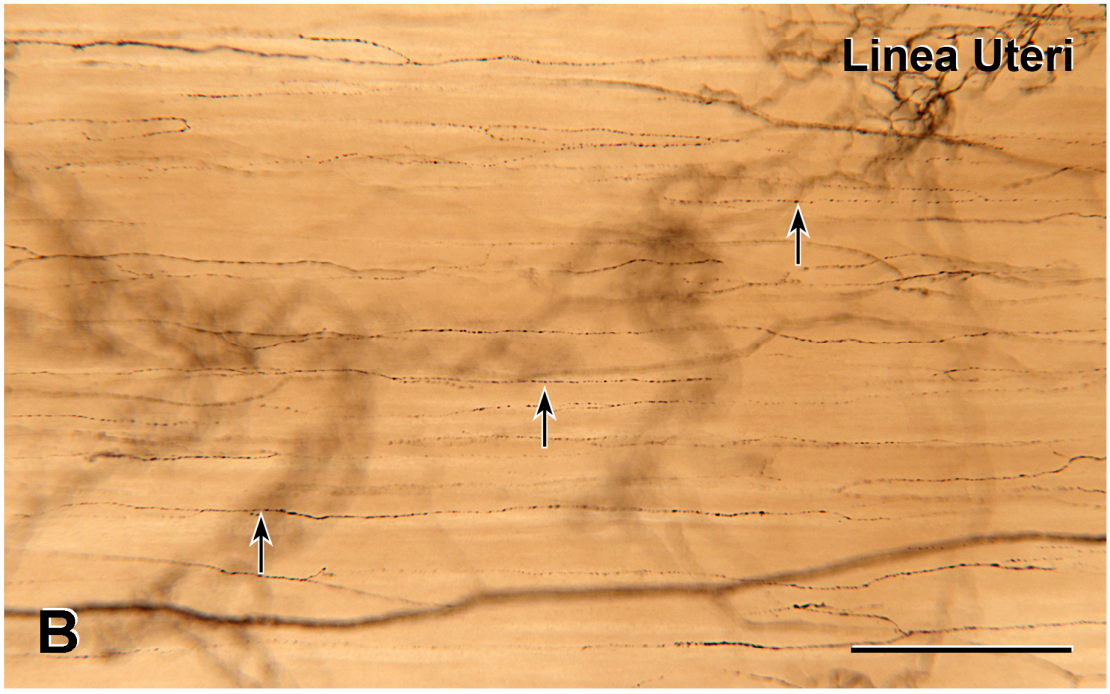

FIGURES 3.3C & 3.3D NPY-immunoreactive axons associated with blood vessels.

C, NPY-immunoreactive axons around blood vessels. Bar, 250 μm. **D**, Higher magnification micrograph of nerve bundle containing NPY around blood vessel. NPY axons (arrow) were followed deep into the endometrium. Bar, 50μm

NPY : Estrous

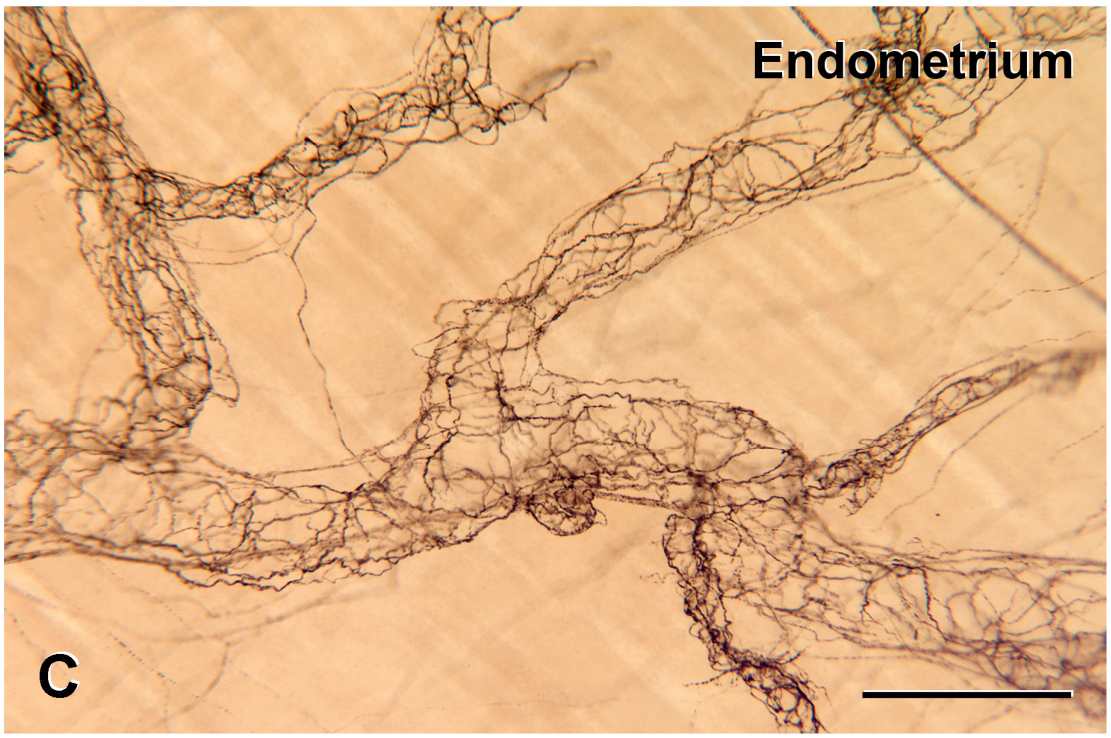

the anti-mesometrial side. These axons were oriented similar to the circular smooth muscle but their exact location in relation to the border between the circular muscle and endometrium could not be determined in the whole mounts. The location of these axons will be revealed by serial paraffin sections cut *en face* and stained with haematoxylin and eosin. Most of these fine varicose NPY axons arose from nerve bundles associated with blood vessels in the myometrium.

NPY innervation of endometrium: The number of NPY-immunoreactive axons associated with blood vessels gradually reduced as the blood vessels reached the endometrium. Varicose NPY-positive axons often left the perivascular plexus to travel to the endometrium where they terminated (Figure 3.3F). Occasionally, NPY axons went back to the myometrium to join another perivascular plexus. Many nerve bundles containing NPY-immunoreactive axons were not associated with blood vessels in the endometrium. Nerve bundles in this location appeared to contain fewer NPY-positive than TH-positive axons. Sometimes, the bundles of NPY axons that were mostly not associated with blood vessels travelled towards blood vessels but did not join the nerve bundles that ran just beside the vessels.

There appeared to be no substantial differences in NPY innervation between the mesometrial and anti-mesometrial sides of the uterus or between the ovarian, middle and cervical regions. However, the fine varicose NPY axons seen at the circular muscle/endometrium boundary only occurred on the mesometrial of the uterus side and were absent in the anti-mesometrial side.

Immunostaining of both right and left uterine horns from one non-pregnant rat showed that NPY innervation did not differ between the right and left horns.

FIGURES 3.3E & 3.3F NPY-immunoreactive axons in the circular muscle and endometrium

E, Fine, varicose NPY-immunoreactive axons (arrows) on the mesometrial side of the non-pregnant uterus. Bar, 250 µm. **F**, NPY-positive axon (arrow) close to a uterine gland deep in the endometrium. Bar, 50µm

NPY : Estrous

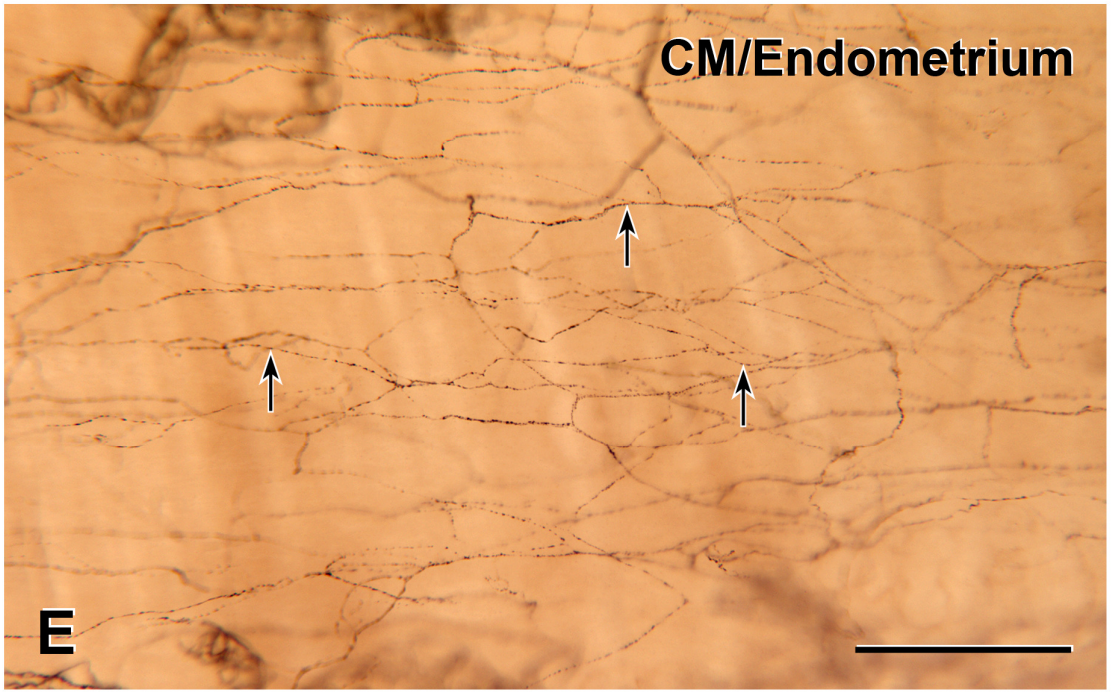

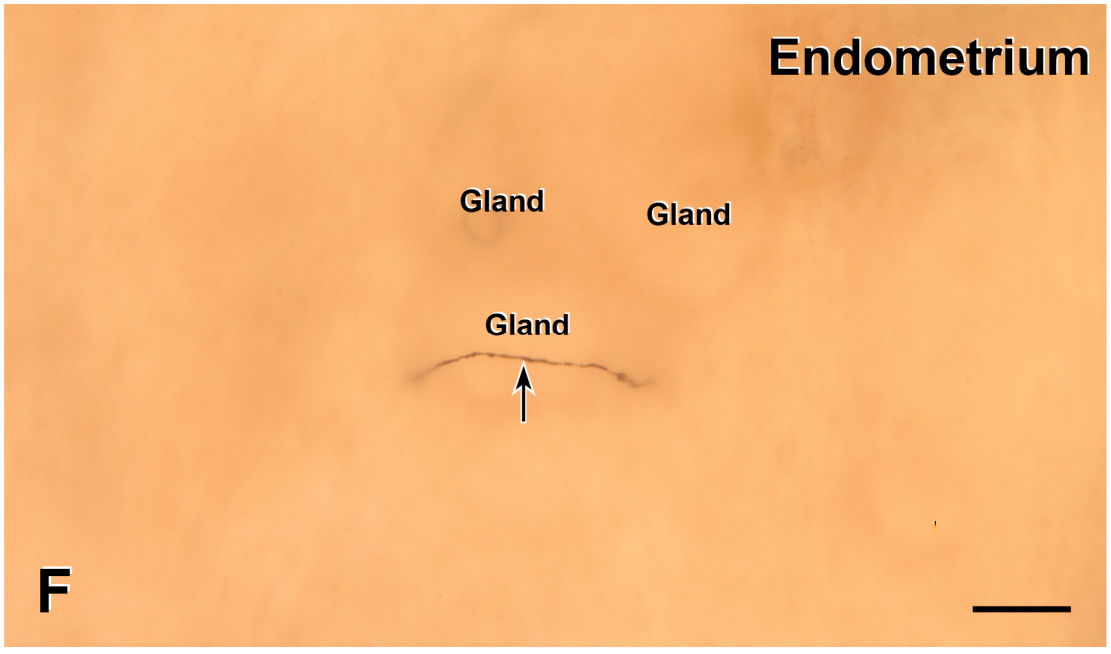

Sensory Innervation of the non-pregnant rat uterus

Immunoreactivity for calcitonin gene-related peptide (CGRP) and substance P (SP) were used to identify sensory nerves. CGRP-immunoreactive axons and SP-immunoreactive axons were found in all layers of the non-pregnant rat uterus at the estrous stage.

Calcitonin Gene-Related Peptide (CGRP)

CGRP-immunoreactive axons moderately innervated blood vessels; this innervation was less dense than the innervation provided by TH- and NPY-immunoreactive axons. Nerve bundles containing non-varicose CGRP-immunoreactive axons entered the uterus along with blood vessels at the mesometrium. Unlike TH and NPY-containing axons, CGRP-positive axons occurred only around the larger blood vessels in the uterus and not around smaller branches. (Figure 3.4C). CGRP-stained axons were associated with fewer blood vessels than TH- or NPY-stained axons. Compared to TH and NPY, the number of CGRP positive axons in nerve bundles associated with blood vessels was also lower (Figure 3.4A).

CGRP innervation of the myometrium: Many varicose CGRP axons were found in the myometrium. Linea uteri had more varicose CGRP axons than the rest of the uterine smooth muscle (Figure 3.3B). Few CGRP-immunoreactive axons were seen in the circular smooth muscle. CGRP axons were oriented predominantly longitudinally in the linea uteri and longitudinal muscle layer and predominantly circularly in the circular muscle layer.

CGRP innervation of the endometrium: CGRP axons were associated with blood vessels in the endometrium and also occurred as free nerve endings. In general, CGRP-positive axons in the endometrium arose from nerve bundles associated with blood vessels

FIGURES 3.4A - 3.4F CGRP innervation of the non-pregnant uterus

A, Whole mount preparation of the entire full thickness non-pregnant uterine horn stained for CGRP. Bar, 5 mm. Letters indicate the location of the micrographs shown in Figures 3.4B-F. Figures B, C and D show different focal planes through the same region of the whole mount in A. **B**, Dense CGRP-immunoreactive axons (arrows) in the linea uteri. Bar, 250µm. **C**, CGRP-positive axons around blood vessels. Bar, 250 µm. **D**, CGRP-containing axons (arrows) travel close to uterine gland deep in the endometrium. Bar, 250 µm. **E**, CGRP-stained axons in the endometrium that are not associated with any identifiable structure. Bar, 250 µm. **F**, CGRP-immunoreactive axons (arrows) very close to a uterine gland. Bar, 100µm.

CGRP : Estrous

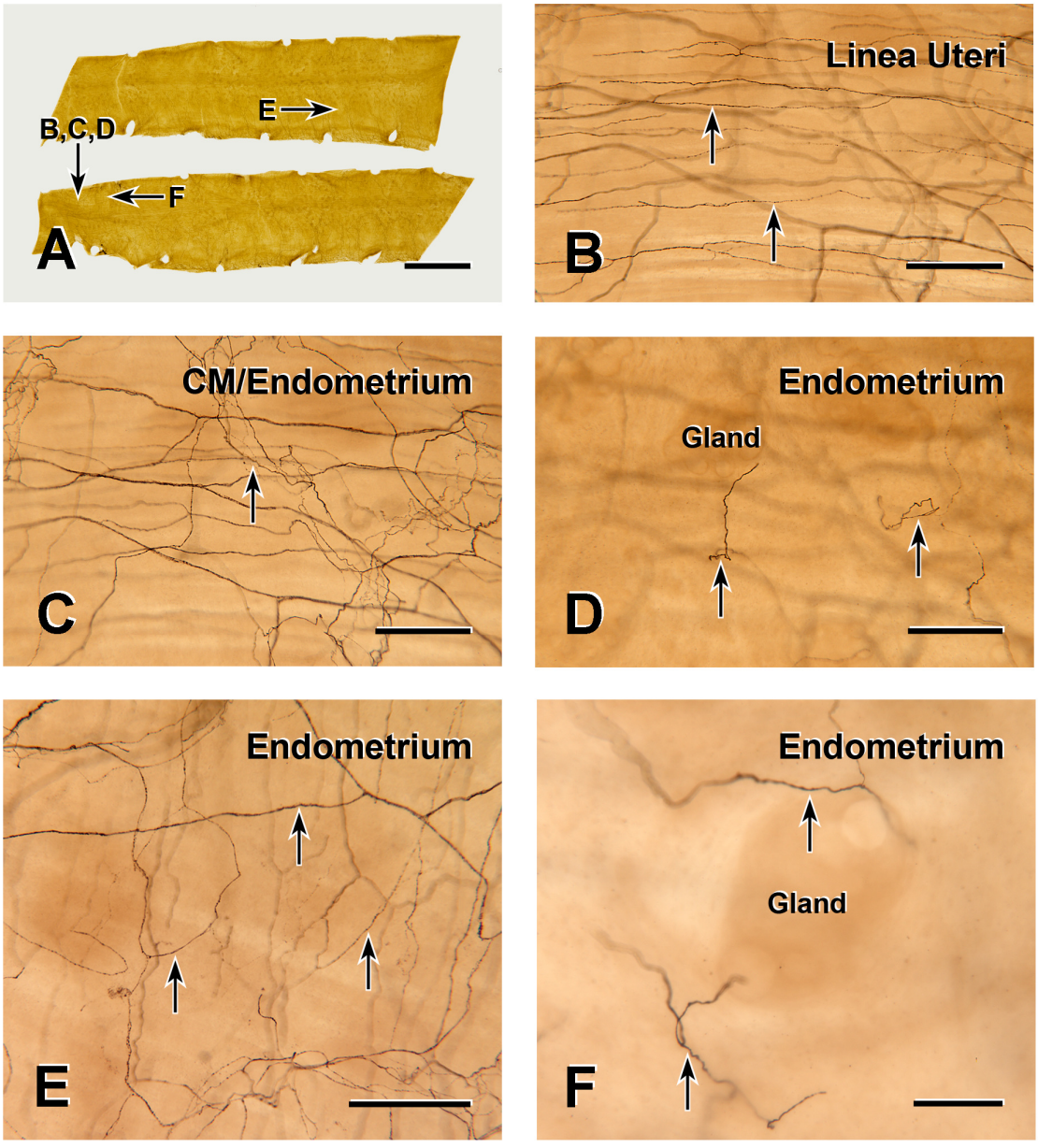

in the myometrium. Many CGRP-immunoreactive axons occurred deep in the endometrium close to the uterine glands (Figure 3.4D & 3.4F). The density of this endometrial CGRP innervation was greater than that of the sympathetic innervation since TH and NPY were only rarely seen near uterine glands. The endometrium was more densely innervated than the muscle. Thick nerve bundles containing CGRP-immunoreactive axons were similar in density to nerve bundles containing NPY-immunoreactive axons. However, there were fewer nerve bundles containing CGRP axons than bundles containing TH-immunoreactive axons. Many varicose and non-varicose CGRP axons wandered freely in the endometrium and did not appear to be associated with blood vessels or any other identifiable anatomical structure. (Figure 3.4E)

The distribution of CGRP-immunoreactive axons did not vary noticeably between the mesometrial and anti-mesometrial sides or between the ovarian, middle and cervical regions of the non-pregnant uterus.

CGRP innervation between left and right uteri of the one non-pregnant rat examined did not show any notable differences.

Substance P (SP)

A few non-varicose SP-immunoreactive axons were found around blood vessels. Nerve bundles containing SP-immunoreactive axons entered the uterus along with blood vessels at the mesometrium. Staining for SP in these nerve bundles was much less compared to TH and NPY staining but similar to CGRP staining (Figure 3.5A). Fewer blood vessels had SP axons associated with them than CGRP axons and many fewer had SP axons associated with them than TH and NPY axons (Figure 3.5C). The number of SP axons in perivascular nerve bundles reduced as the blood vessels approached the anti-mesometrial side of the uterine horn. Similar to CGRP, SP axons were also found only

FIGURES 3.5A – 3.5E SP innervation of the non-pregnant rat uterus.

A, Whole mount preparation of the entire full thickness non-pregnant uterine horn stained for SP... Bar, 5 mm. Letters indicate the location of the micrographs shown in Figures 3-5B-D. Figures C, D and E show different focal planes through the same region of the whole mount in A. **B**, Thick nerve bundle containing SP axons in the endometrium. Bar, 250 µm. **C**, SP axons around blood vessel in the muscle. Bar, 250 µm. **D**, Fine varicose SP axons near the boundary between the circular muscle and the endometrium. Bar, 250 µm. **E**, SP axons deep in the endometrium. Bar, 250 µm.

SP : Estrous

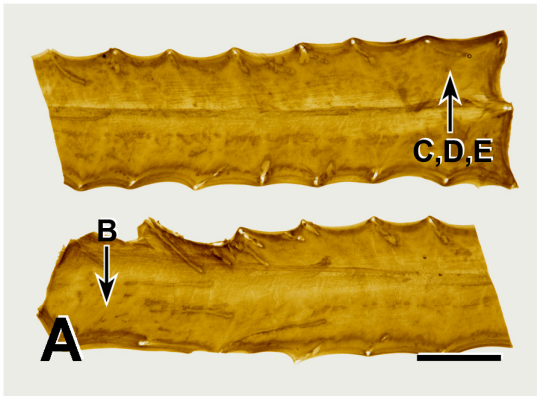

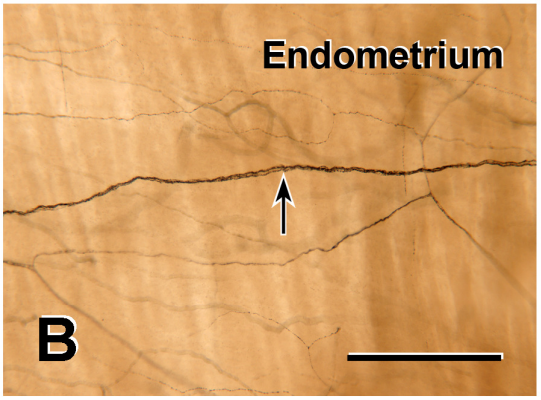

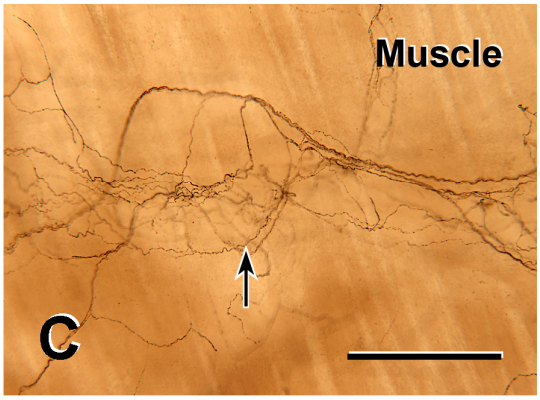

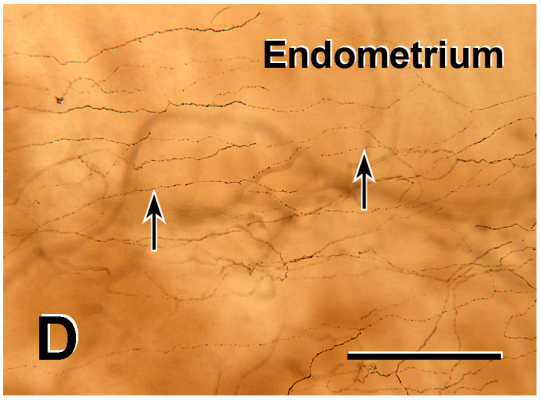

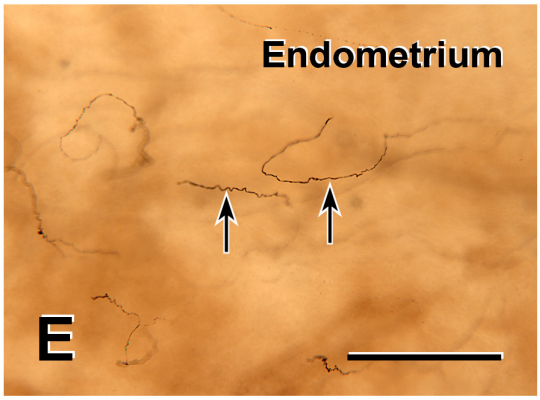

along the larger blood vessels in the uterus and not seen around smaller arterioles that branched off the larger vessels.

SP innervation of the myometrium: Varicose SP-immunoreactive axons were found in the myometrium of the non-pregnant uterus. SP axons were sparse compared to CGRP axons in the myometrium. There was no marked difference in the innervation of the linea uteri compared to the rest of the uterine smooth muscle. Fine, varicose SP-immunoreactive axons occurred in a regular pattern with an orientation similar to the circular smooth muscle cells (Figure 3.5D). Although the arrangement of these axons suggests that they are in the circular smooth muscle, their location cannot be confirmed by assessing whole mounts. Serially sectioned paraffin sections cut *en face* and stained with haematoxylin and eosin will reveal this information. The regular meshwork of fine varicose SP axons was less dense compared to the meshwork of NPY axons. This regular arrangement of axons near the circular muscle-endometrium interface was not seen after staining for CGRP or TH.

SP innervation of the endometrium: SP axons, mostly varicose, were found deep in the endometrium but there were fewer SP- than CGRP-containing axons in this layer. Some varicose SP axons approached uterine glands. These fibers arose from blood vessels in the myometrium. As after staining for NPY or CGRP, there were a few thick nerve bundles containing SP-immunoreactive axons that were not associated with blood vessels. These bundles of SP axons were less frequent and contained fewer immunoreactive axons compared to similar bundles stained for TH. (Figure 3.5B).

SP innervation did not differ between the mesometrial and anti-mesometrial sides of the uterus. However, there appeared to be a slight increase in the density of SP axons in the middle region of the uterus compared to the ovarian and cervical regions.

SP immunoreactivity in both right and left uterine horns of one non-pregnant rat indicated that innervation did not differ between horns.

Parasympathetic innervation of the non-pregnant rat uterus

Immunoreactivity for nitric oxide synthase (NOS) and the vesicular acetylcholine transporter (VAChT) were used to identify parasympathetic nerves. NOS-immunoreactive axons and VAChT -immunoreactive axons were found in all layers of the non-pregnant rat uterus at the estrous stage.

Nitric Oxide Synthase (NOS)

NOS-immunoreactive axons densely innervated blood vessels. NOS-positive axons entered the uterus along with blood vessels at the mesometrium. NOS innervation around blood vessels was less dense than TH or NPY innervation around blood vessels (Figure 3.6B). NOS axons associated with blood vessels were mostly non-varicose; only a few varicose axons were seen. Fewer blood vessels were innervated by NOS axons compared to TH and NPY. (Figure 3.6A).

NOS innervation of the myometrium: Many varicose NOS-immunoreactive axons were seen in the myometrium. NOS innervation was similar in density to SP innervation in the myometrium but sparse compared to TH, NPY and CGRP. There was no notable difference in the NOS innervation of linea uteri compared to the rest of the uterine smooth muscle. Fine varicose NOS-immunoreactive axons were found in a regular pattern along the entire length of the uterus; many of these axons arose from nerve bundles around blood vessels (Figure 3.6C). These fine, varicose, axons were dense and were probably in the

FIGURES 3.6A-3.6D NOS innervation of the non-pregnant rat uterus

A, Whole mount preparation of the entire full thickness non-pregnant uterine horn stained for NOS. Bar, 5 mm. Letters indicate the location of the micrographs shown in Figures 3.6B-D. Figures B and C show different focal planes through the same region of the whole mount in A. **B**, NOS-immunoreactive axons around blood vessel in between the circular and longitudinal smooth muscle layers. Bar, 250 µm. **C**, Fine varicose NOS-positive axons near the boundary of the circular muscle and endometrium. Bar, 250 µm. **D**, Thick nerve bundle containing NOS-positive axons in the endometrium. Bar, 250 µm.

NOS : Estrous

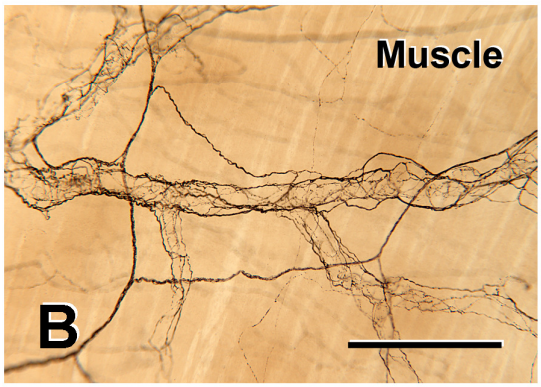

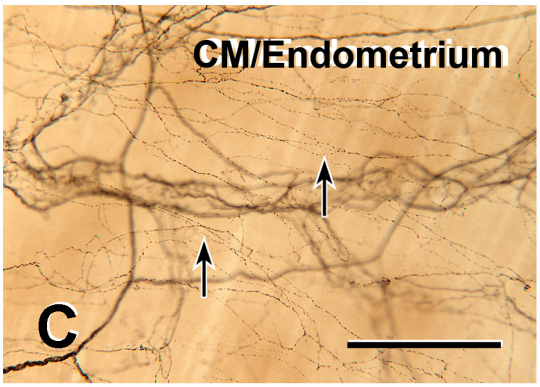

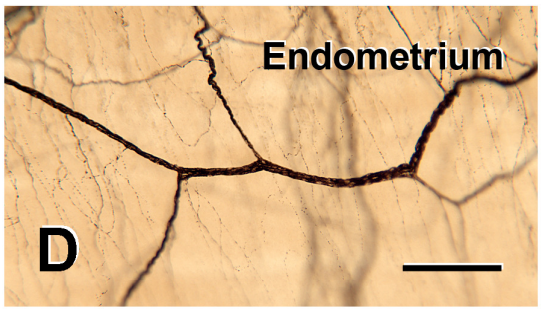

circular smooth muscle due to their orientation. However, serial sections cut on en face and stained with haematoxylin and eosin will be needed to confirm this.

NOS innervation of the endometrium: The density of NOS-immunoreactive axons was higher in the endometrium than in the muscle. The endometrium contained thick nerve bundles containing NOS-immunoreactive axons that not associated with blood vessels; NOS staining in these nerve bundles was more intense that the staining of similarly located thick nerve bundles stained for TH, NPY, SP, CGRP and VAChT (Figure 3.6D). On one occasion, one of these thick nerve bundles containing NOS axons travelled towards a blood vessel and joined a nerve bundles that ran just along side the vessel.

There were some differences in the NOS innervation of the rat uterus along its length and around its circumference. NOS-immunoreactive axons more densely innervated the cervical region of the uterus compared to middle region. NOS innervation was slightly lower in the ovarian region compared to the middle region and was absent at the most distal region of the uterus where the Fallopian tube entered. The fine varicose NOS-containing axons at the circular muscle/endometrium interface were present on the mesometrial but absent on the anti-mesometrial side of the uterus. There was no difference in the density of NOS-immunoreactive axons between the right and left uterine horns as seen in two non-pregnant rats from which both horns were processed for NOS-immunoreactivity.

Vesicular Acetylcholine Transporter (VAChT)

Uterine tissue did not stain well with the antibody against VAChT that was used in this project. The level of background staining was much higher throughout the uterus than with the other antibodies. Non-specific staining of the uterine glands was particularly noticeable.

A few varicose VAChT-immunoreactive axons were seen around blood vessels. Nerve bundles containing VAChT-positive axons entered the uterus along with blood vessels at the mesometrium. The perivascular plexus of VAChT-immunoreactive axons was less dense than the plexus formed by TH- or NPY-stained axons (Figure 3.7A). VAChT-positive axons occurred in thick nerve bundles but there were fewer in each bundle than after staining with TH or NPY. (Figure 3.7B).

VAChT innervation of the myometrium: Many varicose VAChT-immunoreactive axons were seen in the myometrium. There was a slight increase in the density of VAChT-containing axons in the linea uteri compared to the rest of the uterine smooth muscle (Figure 3.7D). VAChT-immunoreactive axons were less dense in the myometrium compared to TH, NPY and CGRP axons but similar in density to SP and NOS. Fine varicose VAChT-positive axons made a regular pattern similar in orientation to the circular smooth muscle; these axons were denser in the cervical region than in the middle and ovarian regions (Figure 3.7C). Serial sections cut en face and stained for haematoxylin and eosin will need to be examined in order to confirm the location of these regularly arranged axons.

VAChT innervation of the endometrium: VAChT-immunoreactive axons were seen around blood vessels and travelling alone in the endometrium. Rare VAChT-positive axons were seen deep in the endometrium but not close to uterine glands.

The fine, varicose VAChT-immunoreactive axons near the boundary between the circular muscle and endometrium occurred only on the mesometrial and not on the anti-mesometrial sides of the uterus. VAChT innervation appeared slightly lower in the ovarian region compared to the middle and cervical regions of the non-pregnant uterus.

FIGURES 3.7A - 3.7C VAChT innervation of the non-pregnant rat uterus

A, Whole mount preparation of the entire full thickness non-pregnant uterine horn stained for VAChT. Bar, 5 mm. Letters indicate the location of the micrographs shown in Figures 3-7B and 3-7C, which show different focal planes through the same region of the whole mount in A. **B**, VAChT-immunoreactive axons around a blood vessel in the muscle. Bar, 250 µm. **C**, Fine varicose VAChT-immunoreactive axons at the circular muscle/endometrium boundary. Bar, 250 µm. **D**, VAChT-immunoreactive axons in the linea uteri. Bar, 250 µm.

VAChT : Estrous

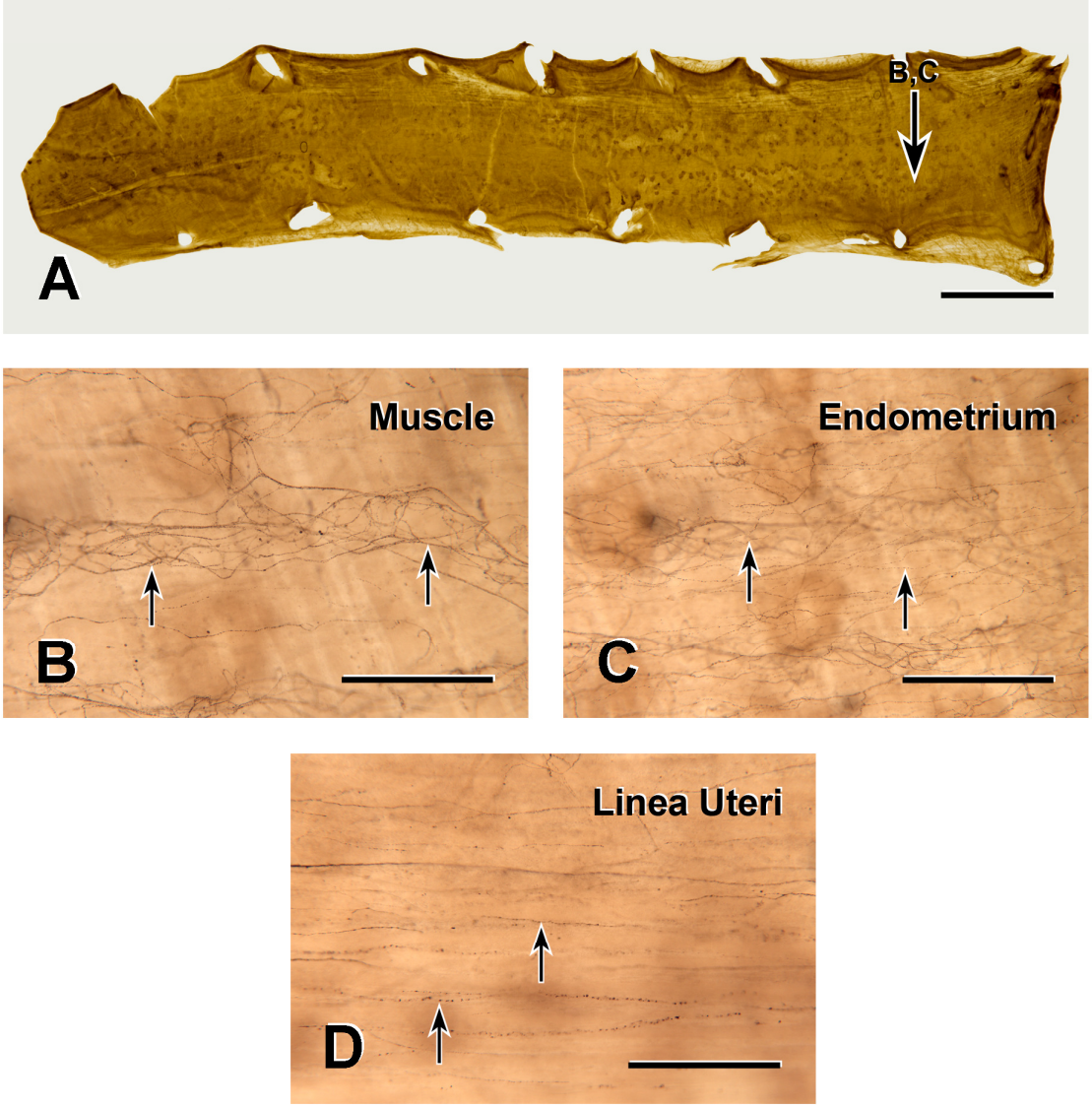

VAChT-immunoreactive axons did not differ in density between the right and left uterine horns when right and left uterine horns from two non-pregnant rats were examined.